Published in final edited form as:
Neuroimage. 2010 November 1; 53(2): 707–717. doi:10.1016/j.neuroimage.2010.06.069.

Multimodal imaging of repetition priming: Using fMRI, MEG, and intracranial EEG to reveal spatiotemporal profiles of word processing

Carrie R. McDonald[1,2], **Thomas Thesen**[2,3], **Chad Carlson**[3], **Mark Blumberg**[3], **Holly M. Girard**[2], **Amy Trongnetrpunya**[3], **Jason S. Sherfey**[2], **Orrin Devinsky**[3], **Rubin Kuzniecky**[3], **Werner K. Dolye**[4], **Sydney S. Cash**[2,5], **Matt K. Leonard**[2], **Donald J. Hagler Jr.**[2,6], **Anders M. Dale**[2,6,7], and **Eric Halgren**[2,6,7]

[1] Department of Psychiatry, University of California, San Diego

[2] Multimodal Imaging Laboratory, University of California, San Diego

[3] Comprehensive Epilepsy Center, Department of Neurology, New York University

[4] Department of Neurosurgery, New York University

[5] Department of Neurology, Massachusetts General Hospital, Harvard Medical School, Boston

[6] Department of Radiology, University of California, San Diego

[7] Department of Neurosciences, University of California, San Diego

Abstract

Repetition priming is a core feature of memory processing whose anatomical correlates remain poorly understood. In this study, we use advanced multimodal imaging (functional magnetic resonance imaging (fMRI) and magnetoencephalography; MEG) to investigate the spatiotemporal profile of repetition priming. We use intracranial electroencephalography (iEEG) to validate our fMRI/MEG measurements. Twelve controls completed a semantic judgment task with fMRI and MEG that included words presented once (new, 'N') and words that repeated (old, 'O'). Six patients with epilepsy completed the same task during iEEG recordings. Blood-oxygen level dependent (BOLD) responses for N vs O words were examined across the cortical surface and within regions of interest. MEG waveforms for N vs O words were estimated using a noise-normalized minimum norm solution, and used to interpret the timecourse of fMRI. Spatial concordance was observed between fMRI and MEG repetition effects from 350–450ms within bilateral occipitotemporal and medial temporal, left prefrontal, and left posterior temporal cortex. Additionally, MEG revealed widespread sources within left temporoparietal regions, whereas fMRI revealed bilateral reductions in occipitotemporal and left superior frontal, and increases in inferior parietal, precuneus, and dorsolateral prefrontal activity. BOLD suppression in left posterior temporal, left inferior prefrontal, and right occipitotemporal cortex correlated with MEG repetition-related reductions. IEEG responses from all three regions supported the timecourse of MEG and localization of fMRI. Furthermore, iEEG decreases to repeated words were associated with decreased gamma power in several regions, providing evidence that

Address for correspondence: Carrie R. McDonald, Multimodal Imaging Laboratory, 8950 Villa La Jolla Drive, Suite C101, La Jolla, CA 92037; ph: 858-534-2678; camcdonald@ucsd.edu.

gamma oscillations are tightly coupled to cognitive phenomena and reflect regional activations seen in the BOLD signal.

Keywords

fMRI; magnetoencephalography; intracranial EEG; memory; language; gamma

INTRODUCTION

Repetition priming has been studied extensively in cognitive neuroscience, but its exact neural correlates remain poorly understood. FMRI studies have demonstrated response suppression, the main neural correlate of priming, in a number of cortical regions following word repetitions. Reliable decreases in blood-oxygen level dependent (BOLD) responses are consistently reported in left ventral occipitotemporal, posterior temporal, and left inferior frontal cortex—regions implicated in word form identification (Allison et al., 1999), lexical access, and semantic processing (Marinkovic et al., 2003; Matsumoto et al., 2005). Repetition of words also has been associated with increased activity in bilateral precuneus, frontoparietal, and hippocampal cortex—regions implicated in resting state and episodic retrieval processes (Weiss et al., 2009). What it not clear from fMRI is precisely *when* repetition effects occur during the course of word processing.

Unlike fMRI, MEG provides a highly accurate picture of the temporal dynamics of cognitive processes, allowing one to visualize repetition effects in real time. MEG studies of priming have revealed reductions in the *N400* response—an event-related field (ERF) implicated in semantic processing—to repeated words from ~350–450ms following word presentation. MEG N400 reductions have been reported in previous studies in similar regions to those identified with fMRI (Marinkovic et al., 2003). In addition, MEG studies have generally revealed priming effects that are more widespread in temporoparietal regions, often extending into the anterior temporal pole—a region not always captured with fMRI due to signal loss (Devlin et al., 2000).

However, neuroimaging methods such as fMRI and MEG rely on noninvasively-recorded responses, which cannot provide unequivocal evidence of local neuronal generators. In addition, it has been suggested that some discrepancies between fMRI and MEG patterns may stem from the fact that that the BOLD signal is closely coupled with power changes in high gamma activity (Lachaux et al., 2007)—a frequency range not always detected at the scalp due to the low amplitude characteristic of gamma waveforms (Dalal et al., 2009), contamination with EMG artifact (Whitham et al., 2008) and microsaccades (Yuval-Greenberg et al., 2008). Increased gamma oscillations have been associated with a number of cognitive processes, including language and memory (Lachaux et al., 2007; Sederberg et al., 2007). Therefore, understanding their local generation may further enhance knowledge of word priming effects. Intracranial electroencephalography (iEEG) is the only current method capable of localizing such sources unambiguously and providing validation of the temporal, spatial, and spectral features of the fMRI and MEG repetition priming effects (Halgren, 2004b).

The goal of this study was to utilize sophisticated multimodal imaging to evaluate the spatiotemporal dynamics of repetition priming. We leveraged the high temporal resolution of MEG and iEEG to examine the time course of regional fMRI activations. In addition, we explored the regions and time windows during which the electromagnetic and hemodynamic priming effects showed the strongest correlation across participants. IEEG recordings were evaluated in regions that showed strong MEG and/or fMRI repetition effects, and the spatiotemporal and spectral features of iEEG responses were analyzed. We hypothesized that

fMRI and MEG would show repetition priming effects in left inferior frontal, ventral occipitotemporal, and superior temporal cortex. We predicted that the regions associated with response suppression in fMRI would show strong correlations with reductions in MEG sources between ~350–450ms—capturing peak N400 effects. We predicted that iEEG recordings would support previous studies demonstrating local generators of the N400 in multiple perisylvian regions (Halgren, 2004a), and that N400 iEEG responses would be particularly evident in the high gamma range.

MATERIALS AND METHODS

Participants

Twelve right-handed, healthy controls between the ages of 19 and 36 (6 males) and six patients undergoing invasive inpatient monitoring at the New York University (NYU) Comprehensive Epilepsy Center for treatment of drug-resistant epilepsy participated in the study. The study was approved by the Institutional Review Board at NYU and each subject's consent was obtained in accordance with the ethical standards promulgated in the Declaration of Helsinki. Handedness in all control participants was assessed with the Edinburgh Handedness Inventory (Oldfield, 1971). MEG and fMRI data were available for all healthy controls, whereas intracranial data only are provided for the patients. Table 1 provides clinical information for the six patients.

Semantic Judgment Task

All twelve healthy controls completed comparable versions of a semantic judgment task for both fMRI and MEG and all patients completed the same semantic judgment task during iEEG recordings. In this task, participants were instructed to respond by pressing a button in response to low-frequency target items (i.e., animals). Task stimuli were presented visually as white letters on a black background in Arial font. Stimuli consisted of 400 novel words that were presented only once, 400 "old" words (20 repetitions of 20 words), 400 consonant letter strings, 400 false font stimuli, and 80 target words (i.e., animals). In order to minimize expectancy effects, repeating words did not occur in the same order each time. All real word stimuli were 4–8 letter nouns, with a written lexical frequency of 3–80 per 10 million (Francis and Kucera, 1982). Data were collected using a rapid stimulus onset asynchrony (SOA; 600ms) and a very large number of trials per condition in order to obtain electrophysiological data with a high signal-to-noise ratio (SNR) in a short time frame. For all three modalities, the experimental task was organized into two separate lists, each list taking approximately 10 minutes to complete. The tasks were programmed using Presentation software (Neurobehavioral Systems, Inc). The order of MEG and fMRI sessions was counterbalanced across healthy controls.

fMRI—A blocked version of the semantic judgment task was designed for fMRI in order to maximize the signal-to-noise ratio (SNR) in regions believed to be involved in lexical-semantic processing, but also known to be susceptible to signal loss (Devlin et al., 2000). Sixty blocks of stimuli were created that included 10 blocks of new words, repeating (old) words, and letter strings, and 30 blocks of false font stimuli (i.e., sensory controls). This design produced 30 active blocks and 30 control blocks. Each block contained 40 words of one stimulus type, plus two target words. Blocks of new words and consonant strings were presented in random order. Blocks of old words were not randomized. Rather, each old word was presented four times in each of the five blocks (i.e., 20 repetitions), and blocks were spaced such that old words only occurred approximately every 5–10 seconds per block and blocks of words repeated every 2–3 minutes. The button response was to low frequency targets (i.e., animals) in each block.

MEG and iEEG—Event-related versions of the semantic judgment task were designed for MEG and iEEG such that each of the old words was presented approximately every 30 seconds

(+/− 10 seconds) and there were on average 42 intervening stimuli between presentations of a given old word. Novel words, consonant strings, and false fonts were presented in random order throughout each list. However, the sequence of stimulus conditions was balanced to ensure that each condition was preceded by every other condition with equal likelihood.

Procedure

MRI acquisition—MRI data were acquired using a 3T Siemens Allegra head-only MRI scanner (TE = 3.25 ms, TR = 2530 ms, TI = 1100 ms, flip angle = 7 deg, FOV = 256 mm, matrix = 256 × 256 × 171, slice thickness = 1.3 mm). Two T1-weighted images were acquired, rigid body registered to each other, and reoriented into a common space, roughly similar to alignment based on the AC-PC line. Images were corrected for non-linear warping caused by non-uniform fields created by the gradient coils. Image intensities were further normalized and made uniform with the FreeSurfer (3.0.5) software package (http://surfer.nmr.mgh.harvard.edu). Functional BOLD data images were acquired using a T2*-sensitive echo planar imaging sequence (TR = 3000ms, TE = 25 ms, flip angle 90 degrees; 3×3×3 voxels; FOV = 192mm). Thirty-nine interleaved transverse slices (3mm width with no gap) were obtained during each TR, covering the entire cortex. The image files in DICOM format were transferred to a Linux workstation for morphometric and functional BOLD analysis.

MRI analysis—Geometric representations of the cortical surface were constructed from the T1-weighted structural volumetric images using procedures described previously (Dale et al., 1999; Fischl et al., 2002; Fischl et al., 1999a). First, segmentation of cortical white matter was performed and the estimated border between gray and white matter was tessellated, providing a topographically correct representation of the surface. This representation of the folded cortical surface was used to derive the locations of the dipoles used in the analysis of the MEG data and visualization of the BOLD response for fMRI. For MEG and fMRI intersubject averaging, the reconstructed surface for each subject was morphed into an average spherical representation, optimally aligning sulcal and gyral features across subjects while minimizing metric distortion (Fischl et al., 1999b). This surface-based deformation procedure results in a substantial reduction in anatomical and functional variability across subjects relative to volume-based normalization approaches (Fischl et al., 1999b).

Functional MRI data were preprocessed using FSL (www.fmrib.ox.ac.uk/fsl). For each subject, motion correction was performed using MCFLIRT (Jenkinson et al., 2002), data were spatially smoothed using a 5 mm full width half-maximum (FWHM) Gaussian kernel, grand-mean intensity normalized, high-pass filtered at sigma = 50 msec and pre-whitened using FILM (Woolrich et al., 2001). Functional scans were co-registered to T1-weighted images (Jenkinson et al., 2002; Jenkinson and Smith, 2001), and analyzed using FMRI Expert Analysis Tool (FEAT) Version 5.90, part of FSLs FMRIB s software library. BOLD parameter estimates (beta-weights) were averaged across the two runs for each contrast of interest (N > O and O > N). Percent signal change was calculated in MATLAB (The Mathworks, Natrick, MA) by multiplying the beta-weights by 100 × the regressor height and dividing by the mean functional volume. Individually averaged functional data were then resampled from each volume to each individual s native surface, then from native surface to spherical atlas space for surface-based group analysis.

Normalized beta-weights (relating to the BOLD amplitude) for the N > O and O < N contrasts were examined across the cortical surface and within group comparisons were performed for each contrast. T-stat maps were generated from the beta-weights, and cluster-based thresholding was performed according to procedures described by Hagler et al. (Hagler et al., 2006). In brief, Gaussian Random Field Theory was used to model the distribution (Worsley

et al., 1996) and the FWHM smoothness of the data was estimated from normalized residuals. This yielded significant clusters of fMRI activity for the O > N and N > O contrasts for the group (FWHM = 8mm, with t-statistics thresholded at $p<.001$ and cortical surface clusters smaller than 94 mm^2 excluded, achieving a corrected cluster $p < 0.05$). In addition, ROI analyses were performed based on clusters of significant functional activity identified in the fMRI data. In each case, a functional label was generated at the group level and mapped from the average subject back to each individual (Fischl et al., 1999a; Fischl et al., 1999b). This yielded the average BOLD response and percent signal change value for each individual and within each ROI.

MEG acquisition—Magnetic fields were recorded by a whole-head Magnes 3600 WH MEG system with 248 magnetometers (4D Neuroimaging, San Diego) in a magnetically-shielded room. Pairs of EOG electrodes were used to detect eye blinks and movements. To ensure head stability, foam wedges were inserted between the subject's head and the inside of the unit and a Velcro strap was placed under the subject's chin. The translation between the MEG coordinate systems and each participant's structural MRI was made using three head position coils placed on the scalp and fiducial landmarks (Hamalainen, 1993). Signals were recorded continuously with 1017 Hz sampling rate and minimal on-line filtering (.1–200 Hz). Data were then low-pass filtered off-line at 40 Hz (transition band = 4 Hz), high-pass filtered at .2 Hz (transition band = .4 Hz), detrended, baseline corrected, and downsampled by a factor of four before separate averages were created for each subject. Epochs containing EOG amplitudes exceeding 280 microvolts in the EOG electrode or magnetometer amplitudes exceeding approximately 3000 fT were excluded from the averages. Grand averages for each stimulus type were created by averaging across the two runs.

MEG source analysis—To estimate the time courses of cortical activity, distributed source estimates were calculated from magnetometer data using dynamic statistical parametric mapping (dSPM) (Dale et al., 2000). This method is based on the assumption that the main generators of MEG and EEG signals are localized in the gray matter. Once the exact shape of the cortical surface is known, this information can be used to reduce the MEG solution space. Furthermore, normalization procedures are used that take into account the noise sensitivity at each spatial location, allowing for statistical parametric maps that provide information about the estimated signal at each location relative to the noise. First, the cortical surface was subsampled to about 2500 dipole locations per hemisphere (Dale et al., 2000). Second, the forward solution at each location was calculated using boundary element method (Oostendorp and Van Oosterom, 1992). Third, dipole power was estimated at each cortical location every 4 ms and divided by the predicted noise power obtained from all conditions for each individual. This method generates statistical maps that are square root of *F* distributed and represent the activity for each participant throughout the time course. These values were then averaged on the cortical surface across individuals after aligning their sulcal-gyral patterns (Dale and Halgren, 2001). From the mean group activity maps, thresholded t-stat maps were calculated that take into account within-group variability and the same cluster based-thresholding approach used for the fMRI analysis was performed on selected time frames for the MEG data (FWHM = 22mm; t-statistics thresholded at $p<.001$ and cortical surface clusters smaller than 257 mm^2 excluded; corrected cluster $p < 0.05$). Three time windows were selected based on previous MEG (Dhond et al., 2001; Marinkovic et al., 2003) and intracranial (Halgren et al., 1994; Halgren et al., 2006) studies of semantic and repetition priming that have revealed the approximate time course associated with lexical access (~200–240ms), semantic processing (~350–450ms), and conscious recollection (~500–600ms). The last time window was of interest because previous studies have demonstrated late repetition effects that occur ~540ms, even in the context of incidental memory tasks (Dale et al., 2000). Finally, ROI analyses were performed using the ROIs derived from the fMRI surface maps. By using identical surface-

based ROIs, statistical maps (t-stats), and methods for surface-based clustering of the data, we sought to optimize comparisons between our MEG and fMRI results. MEG waveforms across the entire 0–600ms timecourse were extracted from each of the surface-based ROIs.

iEEG acquisition—iEEG data were recorded from six patients undergoing invasive monitoring. Each patient was implanted with 96 to 208 clinical electrode contacts in the form of grid, strip and/or depth arrays. EEG activity was recorded from .1 to 130 Hz (3dB down) using Nicolet clinical amplifier and digitized at 400 Hz, or from 0.6 to 1000 Hz and digitized at 2000 Hz using a custom NSpike recording system (see supplementary figure). Placement of electrodes was based entirely on clinical considerations for identification of seizure foci, as well as eloquent cortex during stimulation mapping. Consequently, a wide range of brain areas was covered, with coverage extending widely into non-epiletogenic regions. Electrode localization was computed by co-registering two T1-weighted MRIs, one obtained preoperatively and one on the day after implant surgery with the electrodes in place. A spatial optimization algorithm was used to integrate additional information from the known array geometry and intra-operative photos to achieve high spatial accuracy of the electrode locations in relation to the cortical MRI surface created during Freesurfer reconstruction.

iEEG analysis—iEEG was down-sampled to 400Hz if necessary and epoched using 500ms before and 1000ms after each stimulus. Data were analyzed in Matlab using the Fieldtrip software package (http://www.ru.nl/fcdonders/fieldtrip/) and custom analysis and visualization routines. For ERP analysis, post-processing steps included a bandpass-filter at .1–30Hz, detrending and baseline correction. Epochs containing artifacts were identified by visual inspection of band-pass filtered data and were excluded from further time- and frequency-domain analysis. Raw data were transformed from the time-domain to the time-frequency domain using the complex Morlet wavelet transform (Lachaux et al., 1999). Constant temporal and frequency resolution across target frequencies was obtained by adjusting the wavelet widths according to the target frequency. The wavelet widths increase linearly from 14 to 38 as frequency increases from 70Hz to 190Hz, resulting in a constant temporal resolution (σ_t) of 16ms and frequency resolution (σ_f) of 10Hz. For each epoch, spectral power was calculated from the wavelet spectra, normalized by the inverse square frequency to adjust for the rapid drop-off in the power spectrum with frequency, and averaged from 70Hz to 190Hz, excluding line noise harmonics. Visual inspection of the resulting high gamma power waveforms revealed additional artifacts not apparent in the time-domain signal, and the artifactual epochs were excluded from the gamma power analysis. Both ERP and gamma waveforms were compared across stimulus types using a nonparametric randomization test with temporal clustering to correct for multiple comparisons (Maris and Oostenveld, 2007).

Statistical Analysis

Functional MRI t-stat cluster maps for the N > O and O > N contrasts were compared to the tstat cluster maps generated for MEG of the N vs O difference waveform at each of the three time windows of interest. To examine the time course of regional priming effects, time window × condition repeated measures (RM) ANOVAs were performed on the average source estimates within each ROI and hemisphere. To explore the relationship between the hemodynamic and electromagnetic repetition priming effects, Spearman correlations were performed between fMRI percent signal change and modulation of the MEG difference waveform within each ROI and time window. Percent signal change was selected due to evidence that this measure of the BOLD response correlates with N400 priming effects in EEG studies (Matsumoto et al., 2005).

RESULTS

Figure 1 displays cluster-based t-stat surface maps of the N > O (red-yellow) and O > N (blue-cyan) contrasts for fMRI (left panel) and the N vs O difference waveform (red-yellow) for MEG time windows of interest (right panel). Figure 2 portrays the same fMRI cluster maps, with MEG timecourses extracted from significant ROIs identified on the fMRI surfaces.

fMRI

Prominent repetition-related effects for fMRI were observed within 16 regions in the left or right hemisphere. For the N > O contrast, significant clusters were observed in the left inferior prefrontal extending into the precentral gyrus, pars orbitalis, posterior superior temporal, middle temporal, parahippocampal, and superior medial frontal, as well as in bilateral entorhinal, lateral occipitotemporal, and ventral occipitotemporal cortex that extends into anterior fusiform on the left. In addition, O > N responses were observed within bilateral dorsolateral prefrontal cortex, precuneus, inferior parietal/supramarginal cortex. Average percent signal change for the N > O and O < N responses are provided for each ROI in Table 2.

MEG

Cluster-thresholded surface maps of the MEG O vs N difference waveform revealed a dynamic pattern of activity that was observed primarily in bilateral orbital and ventral occipitotemporal cortex early on (~80–120ms), followed by repetition effects from ~200–240ms in the superior temporal cortex bilaterally, left dorsolateral prefrontal, inferior parietal, and left ventral occipitotemporal regions. Inspection of the waveforms in Figure 2 reveals that this early activity is greater for O relative to N words across most regions and may reflect a temporal advantage for processing repeating word stimuli (Marinkovic et al., 2003). This pattern of activity appears increasingly left lateralized from 350–450ms, and is characterized by greater responses to N relative to O words, consistent with modulation of the N400 response to repeated stimuli. In particular, prominent clusters of activity were observed within left inferior prefrontal, left superior, middle, and inferior temporal regions, left ventral occipitotemporal (lingual and fusiform), left temporal pole, left entorhinal, left parahippocampal, and left inferior parietal cortex including parts of the angular and supramarginal gyri. In addition, activity is observed within the right lateral and ventral occipitotemporal cortex (mostly lingual). By ~500–600ms, activity is seen within many of the same regions and again appears more bilaterally distributed.

To estimate the time course within selected ROIs, time by condition RM ANOVAs were performed (see Figure 2). Within the left hemisphere, time by condition interactions were observed within the ventral occipitotemporal [$F(2, 22) = 3.8$, $p < .05$)], superior temporal [$F(2, 22) = 3.7$, $p < .05$)], middle temporal [$F(2, 22) = 4.7$, $p < .05$], pars orbitalis [$F(2, 22) = 3.8$, $p < .05$)], supramarginal [$F(2, 22) = 4.0$, $p < .05$)], inferior frontal [$F(2, 22) = 3.9$, $p < .05$)], entorhinal [$F(2, 22) = 4.1$, $p < .01$)], parahippocampal [$F(2, 22) = 3.5$, $p < .05$)], and temporal pole [$F(2, 22) = 3.8$, $p < .05$)]. Within the right hemisphere, time x condition interactions were observed in the right ventral occipitotemporal only [$F(2, 22) = 3.4$ $p < .05$)]. In each case, new words produced greater responses than old words, but only in the 350–450ms time window. Despite a trend for O > N word responses in the left and right dorsolateral prefrontal and superior temporal ROIs in the 500–600ms time window and across many regions in the 200–240ms time window (p-values between .05 and .10), none of the O > N comparisons reached statistical significance at the ROI level.

fMRI/MEG correlational analysis

Visual inspection of the surface maps and ROI waveforms reveals that the fMRI N > O effect most closely resembles the MEG 350–450ms time window, presumably representing modulation of the N400 effect. In order to examine the relationship between the electromagnetic N400 and hemodynamic priming effects, Spearman correlations were calculated across subjects for each ROI between fMRI percent signal change values and MEG difference waveform values within each time window. Correlational analysis revealed a positive relationship between fMRI N > O and MEG N vs O responses in the left inferior prefrontal ($r = .72$, $p < .01$), left superior temporal ($r = .53$, $p < .05$) and right ventral occipitotemporal ($r = .56$, $p < .05$) ROIs, but only within the 350–450ms time window. Despite similar spatial patterns of activity between MEG and fMRI at the surface level in other ROIs and time windows, the magnitude of the BOLD signal change did not correlate with the modulation MEG waveforms in other regions across individual subjects.

Intracranial validation of MEG/fMRI repetition effects

Inverse methods for source localization based on MEG and fMRI require unproven a priori assumptions. In contrast, it is possible to demonstrate local generation from intracranial recordings without ambiguities. Thus, we also sampled responses to N vs O words from intracranial recordings obtained in six patients. Event-related potentials and high gamma frequency analyses were performed on all patient responses. Table 3 summarizes the number of patients showing locally generated iEEG repetition effects within the 350–450 and 500–600ms time windows.

Event-related potential analysis

Figure 3 shows examples of localized ERPs from four patients based on iEEG recordings. Of our six patients, four had grid coverage of the left posterior superior temporal gyrus/sulcus. Two of the four patients showed a locally generated N > O response between 350–500ms in the vicinity of the left posterior superior temporal region in or near Wernicke's area (Patients A and E). One patient showed an O > N response in the same region that peaked at 600ms following stimulus presentation (Patient D). Only three patients had grids covering the left inferior frontal region near pars opercularis. Two of the three patients demonstrated a N > O response that peaked between 400–500ms following stimulus presentation (Patients B and D). Five of six patients had grid coverage of the lateral occipitotemporal region, either on the left (N = 4) or right (N = 1). Two of the four with left coverage showed a N vs O difference in lateral occipitotemporal cortex that peaked between 350–500ms (Patients A and E). The patient with right coverage showed a similar ERP response in right lateral occipitotemporal cortex (Patient C). Five patients had at least partial coverage of the ventral occipitotemporal region (Left = 3; Right = 2), with one showing N vs O differences on the left (Patient A) between 350–400ms and two patients showing a N > O response on the right (Patients C and F) between 400–600ms in this region. Four patients had partial coverage of the left dorsolateral prefrontal cortex. Two of these patients had strips extending into superior medial frontal cortex on the left. Of the four with left dorsolateral prefrontal coverage, one demonstrated N > O responses between 350–450ms (Patient E). The same patient also demonstrated O > N responses between 500–700ms in left dorsolateral prefrontal cortex. One patient had right dorsolateral prefrontal coverage and demonstrated a N > O response between 500–600ms (Patient F). In addition, one patient with coverage of the left superior medial frontal region showed a local N > O response between 350–450ms (Patient A).

Time course of high gamma (70–190 Hz) power

In addition to the ERP analysis, high gamma responses between 70–190 Hz were sampled in all six patients from the same electrode locations as the ERPs (see examples in Figure 4). High

gamma activity was selected to investigate whether or not gamma oscillations show stronger co-localization with fMRI repetition effects than ERPs in one or more regions, as well as to interpret the valence of our ERP responses. Statistical analysis revealed gamma power differences to N vs O words in the left superior temporal region in two patients (Patients A and E). In one patient, increased gamma power was associated with N > O words that peaked at 400ms (Patient A), whereas the other patient showed O > N increases in gamma that peaked at 500ms (Patient D). In both cases, the gamma oscillations supported ERPs generated at or near the same electrode location. Three patients showed high gamma differences in lateral occipitotemporal cortex (Patients C, D, and E; two left and one right). Of these responses, N > O differences were seen in two patients that began ~300ms following word presentation (Patients C and D). In the other patient, O > N gamma differences were observed later in the time course, peaking around 500ms (Patient E). Three patients showed increased gamma in ventral occipitotemporal cortex (Patients A, C, and F; one left and two right). In all cases, increased gamma oscillations peaked between 400–500ms and reflected N > O responses. Two patients showed increased gamma for N > O words in left dorsolateral prefrontal (Patients A and D) associated with the N400 responses in the ERP data. In addition, increased gamma for O > N words was observed in the left dorsolateral prefrontal cortex in three patients (Patients A, B, and D) and left superior medial/anterior cingulate cortex in one patient (Patient D) from ~500–700ms post-stimulus, associated with late repetition effects.

DISCUSSION

Using advanced multimodal imaging, we demonstrate spatial concordance between fMRI and MEG N400 priming effects within left inferior prefrontal extending into precentral, left posterior superior temporal, left medial temporal, right lateral occipitotemporal, and bilateral ventral occipitotemporal cortex, encompassing much of the lingual and fusiform cortex on the left. We also provide iEEG validation of our MEG/fMRI responses in key regions in multiple patients and reveal co-localization between increased gamma power in iEEG and the fMRI BOLD response. Table 4 summarizes regions of spatiotemporal concordance associated with repetition priming across all three modalities. As can be seen, these priming patterns were largely characterized by reduced responses to repeated words, suggesting facilitation of word processing that is measurable in the hemodynamic and electromagnetic signals.

Furthermore, fMRI revealed repetition enhancement in which repeated words produced greater responses relative to new words in bilateral dorsolateral prefrontal, precuneus, and inferior parietal/supramarginal cortex. Although the MEG ROI analysis indicates a late (~500–600ms) trend for an O > N effects within these ROIs that exceeded our cluster threshold in the surface maps, the condition contrasts did not reach significance at the ROI level. This may be due to our short trial length (i.e., 600ms), which precluded a complete analysis of the late repetition effects that often persist until 700–800ms (Dale et al., 2000). This late effect has been referred to as the LPC/P3b and may reflect conscious recollection of the repeated words. This has been described previously in incidental memory tasks with a large number of repetitions (Dale et al., 2000), presumably because word repetitions become apparent to the participant. In addition, the MEG surface maps reveal significant O vs N differences within left ventral occipitotemporal and bilateral superior temporal clusters between 200–240ms that appear to reflect early, transient enhancements to repeated stimuli, as reported in previous MEG studies of visual word processing (Dhond et al., 2001; Marinkovic et al., 2003). Although these N vs O effects were not significant in the ROI analysis during the early time window, inspection of the waveforms reveals a trend toward O > N responses across several ROIs. Evidence for O > N activity within these ROIs was not captured by fMRI and it has been suggested that the transient nature of the early O > N response is not robust enough to overcome the sustained N > O response that dominates the fMRI BOLD response in these same regions (Marinkovic et al., 2003).

Correlational analysis between our fMRI and MEG repetition priming effects across individuals revealed that fMRI BOLD suppression correlated with MEG priming effects from 350–450ms, but only within the left inferior prefrontal, left superior temporal, and right occipitotemporal region. Repetition suppression within each of these regions has been reported in previous neuroimaging studies of word and object priming (Marinkovic et al., 2003; Schacter and Buckner, 1998). Our within-subject, multimodal fMRI/MEG analysis provides further evidence that these regional priming effects are robust across imaging modalities. Although the relationship between electromagnetic and hemodynamic response changes is complex, a direct correlation between BOLD signal change and N400 modulations has been observed with EEG within the vicinity of the left superior temporal gyrus (Matsumoto et al., 2005). We extend the literature by demonstrating fMRI-MEG correlations within other perisylvian regions implicated in the N400 effect and by providing validation from iEEG of their local generation.

Recent neuroimaging research has demonstrated that repetition suppression across neocortical regions is unlikely to reflect a unitary process. Rather, there is convincing evidence that repetition priming involves multiple component processes with partially unique anatomical substrates. Whereas early response suppression within bilateral occipitotemporal regions likely reflects a “sharpening” of neural activity in response to the perceptual attributes of the stimulus (Fiebach et al., 2005; Schacter and Buckner, 1998) and visual word form priming (Cohen et al., 2002), the late effects (> 300ms) identified in our MEG responses suggest significant top-down influences that may reflect general attention-dependent priming for conceptual information (Klaver et al., 2007). This top-down interpretation is supported by iEEG ERP and/or high gamma recordings in 5 of 6 patients who showed late N > O responses in left or right occipitotemporal cortex in or near regions showing strong activation in fMRI and MEG. This late N > O effect in occipitotemporal cortex has not been previously reported across all three modalities and provides evidence that priming effects within extrastriate cortex are influenced by both feedforward and feedback mechanisms.

In addition, response suppression within left posterior temporal cortex has been attributed to facilitation of lexical access (Matsumoto et al., 2005) or recoding of a written word into a lexical representation (Klaver et al., 2007). This component of repetition priming appears to be independent of the earlier perceptual effects, and may represent automatic, spreading activation of a word s representation. Our data demonstrate response suppression within left temporal cortex in fMRI and in the MEG waveforms that is highly lateralized and sustained after ~250ms. This time period is congruent with other studies that have identified a lexical-processing stage that may represent a transitional stage between perceptual and conceptual priming (Marinkovic et al., 2003). However, the sustained effects observed in these regions in the MEG surface maps and waveforms indicate that left temporal regions also contribute to the main N400 component of repetition priming.

Response suppression within the left inferior prefrontal region is generally believed to reflect conceptual priming, including a reduced demand for semantic memory retrieval (Wagner et al., 2001) and/or facilitation of response selection (Thompson-Schill et al., 1997). Our MEG and fMRI data show response suppression in the left inferior frontal cortex that appears to evolve somewhat latter than the priming effects observed in posterior temporal cortex and is maximal between 350–450ms (i.e., peak N400 effect). The sustained response suppression in left temporal regions during this time supports the notion that left lateral temporal cortex is important for initial lexical access, as well as interactions with prefrontal regions during semantic memory retrieval (Gold and Buckner, 2002). Inspection of the iEEG waveforms provides evidence of locally-generated N400 responses within the left posterior superior temporal and left inferior prefrontal cortex (i.e., in or near Wernicke’s and Broca’s areas) that support our fMRI and MEG N400 reductions and represent core anatomical substrates of conceptual priming.

Taken together, our data provide evidence that the main repetition priming effects seen in fMRI BOLD responses are those associated with the MEG N400 reductions, and not necessarily with the more transient early or late repetition effects that are apparent in the MEG waveforms. This is consistent with previous findings that iEEG/MEG and BOLD responses correlate reasonably well for the N400, but not as strongly with the scalp P3b/LPC (Halgren, 2004b). However, our iEEG data did reveal O > N late repetition effects in left dorsolateral prefrontal cortex in all four patients with recordings sampled from this region that peaked between 500–600ms and may reflect LPC/P3b effects. In three patients, the responses were observed in iEEG high gamma responses but not in the ERPs, suggesting that the BOLD effect associated with conscious recollection may be tightly coupled to increased power in the high frequency ranges not always captured with MEG or ERP measurements (Jerbi et al., 2009; Yuval-Greenberg et al., 2008).

The exact relationship between the BOLD response and increased gamma oscillations observed in cognitive tasks in not entirely known, but memory formation has been associated with increased gamma oscillations recorded with iEEG in left temporal and prefrontal regions (Sederberg et al., 2007). We extend the literature by demonstrating an association between increased gamma power and word priming effects in the context of an incidental memory task. Furthermore, we report increased gamma power for N > O responses in numerous patients in ventral and lateral occipitotemporal, inferior prefrontal, superior temporal, and medial prefrontal cortex that are also reflected in our fMRI activations—many of which were not observed in the ERP data. These findings are consistent with an emerging literature demonstrating that gamma power co-localize with BOLD variations across numerous cortical regions during lexico-semantic tasks (Lachaux et al., 2007), presumably due to its correlation with local neuronal firing (Manning et al., 2009).

In this study, we provide multimodality evidence for the spatiotemporal profile of repetition word priming using fMRI/MEG with support from iEEG recordings. However, there are several limitations to our study that should be noted. First, whereas our MEG and iEEG tasks were event-related, we used a blocked version of the same task for fMRI. A blocked design was selected in order to increase the SNR, optimizing our ability to detect very subtle BOLD changes associated with repetition priming in anterior and ventral temporal lobe regions that are known to be susceptible to signal loss (Chee et al., 2003; Dale et al., 2000). Although numerous studies have reported highly similar patterns of activations between blocked and event-related fMRI designs using lexical-semantic tasks (Chee et al., 2003; Pilgrim et al., 2002; Wagner et al., 2005; Weiss et al., 2009), blocked presentation of items may induce strategies or lead to greater levels of habituation in some regions relative to event-related designs. This may explain the bilateral precuneus and lateral occipitotemporal activations seen in our fMRI data that were not apparent with MEG. Greater BOLD responses to repeated stimuli have been reported previously in bilateral precuneus (Horner and Henson, 2008)—a region implicated in episodic retrieval (Wagner et al., 2005) and task difficulty/workload (Korsnes et al., 2008; Scheibe et al., 2006). It is unclear in our study whether the fMRI responses observed in this region reflect conscious recollection of previous items or the lower task demands introduced by our blocked presentation. However, the presence of lateral occipitotemporal repetition effects in our iEEG recordings that co-localize with the fMRI activations suggest that task design differences are unlikely to account for the occipitotemporal findings. Although using identical task designs for fMRI and MEG/iEEG would appear ideal, there are possible limitations to this approach as well. Had we implemented an event-related fMRI design, we may have reduced our SNR and failed to detect subtle task effects in the anteriormedial temporal lobe that appear to be involved in repetition priming. Alternatively, we could have designed an event-related fMRI design with a higher number of trials per condition to increase the SNR. However, this would have resulted in a greater number of repetitions in our fMRI task relative to MEG and iEEG tasks. The number of repetitions has

been shown to influence priming effects (Ostergaard, 1998), introducing another confound. Despite task differences, the high spatial correlation across imaging modalities in many critical regions suggests that most of the repetition priming effects were robust to differences in the task design.

Second, we used a very brief SOA (i.e, 600m.s.) in order to increase our SNR by allowing for a large number of averages across task conditions in a relatively short time. This brief SOA diminished our ability to fully evaluate very late MEG repetition effects that generally peak around 600 to 700ms post-stimulus. Finally, it is important to note that iEEG data are acquired from patients who are undergoing evaluation for surgical resection of an epileptic focus. Therefore, many of the iEEG responses were sampled near diseased tissue, and the area sampled in each patient varies and is limited to the details of the electrode placement. These are well-known limitations of iEEG research that cannot be avoided. As is accepted practice in iEEG research (Jerbi et al., 2009), we sought to minimize the effects of brain pathology in our iEEG responses by eliminating electrodes from which ictal or interictal discharges were recorded. However, it is still possible that one or more of these factors mitigated our ability to record clear N400 or LPC effects in some of the patients or consistently across regions. Nevertheless, we were still able to detect local repetition priming effects with iEEG in one or more patients that supported the temporal and spatial patterns detected with our non-invasive measures. Multimodal imaging data such as these provide unique insight into the timing, location, and spectral features of cognitive processes, such as repetition priming, and demonstrate the validity of using non-invasive measures for understanding complex brain functions.

Supplementary Material

Refer to Web version on PubMed Central for supplementary material.

Acknowledgments

The work was supported by National Institutes of Health (NIH) Grant K23NS056091 (C.R.M) and NS18741 (E.H.).

References

Allison T, Puce A, Spencer DD, McCarthy G. Electrophysiological studies of human face perception. I: Potentials generated in occipitotemporal cortex by face and non-face stimuli. Cereb Cortex 1999;9:415–430. [PubMed: 10450888]

Chee MW, Venkatraman V, Westphal C, Siong SC. Comparison of block and event-related fMRI designs in evaluating the word-frequency effect. Hum Brain Mapp 2003;18:186–193. [PubMed: 12599276]

Dalal SS, Baillet S, Adam C, Ducorps A, Schwartz D, Jerbi K, Bertrand O, Garnero L, Martinerie J, Lachaux JP. Simultaneous MEG and intracranial EEG recordings during attentive reading. Neuroimage 2009;45:1289–1304. [PubMed: 19349241]

Dale AM, Fischl B, Sereno MI. Cortical surface-based analysis. I. Segmentation and surface reconstruction. Neuroimage 1999;9:179–194. [PubMed: 9931268]

Dale AM, Halgren E. Spatiotemporal mapping of brain activity by integration of multiple imaging modalities. Curr Opin Neurobiol 2001;11:202–208. [PubMed: 11301240]

Dale AM, Liu AK, Fischl BR, Buckner RL, Belliveau JW, Lewine JD, Halgren E. Dynamic statistical parametric mapping: combining fMRI and MEG for high-resolution imaging of cortical activity. Neuron 2000;26:55–67. [PubMed: 10798392]

Devlin JT, Russell RP, Davis MH, Price CJ, Wilson J, Moss HE, Matthews PM, Tyler LK. Susceptibility-induced loss of signal: comparing PET and fMRI on a semantic task. Neuroimage 2000;11:589–600. [PubMed: 10860788]

Dhond RP, Buckner RL, Dale AM, Marinkovic K, Halgren E. Spatiotemporal maps of brain activity underlying word generation and their modification during repetition priming. J Neurosci 2001;21:3564–3571. [PubMed: 11331385]

Fiebach CJ, Gruber T, Supp GG. Neuronal mechanisms of repetition priming in occipitotemporal cortex: spatiotemporal evidence from functional magnetic resonance imaging and electroencephalography. J Neurosci 2005;25:3414–3422. [PubMed: 15800196]

Fischl B, Salat DH, Busa E, Albert M, Dieterich M, Haselgrove C, van der Kouwe A, Killiany R, Kennedy D, Klaveness S, Montillo A, Makris N, Rosen B, Dale AM. Whole brain segmentation: automated labeling of neuroanatomical structures in the human brain. Neuron 2002;33:341–355. [PubMed: 11832223]

Fischl B, Sereno MI, Dale AM. Cortical surface-based analysis. II: Inflation, flattening, and a surface-based coordinate system. Neuroimage 1999a;9:195–207. [PubMed: 9931269]

Fischl B, Sereno MI, Tootell RB, Dale AM. High-resolution intersubject averaging and a coordinate system for the cortical surface. Hum Brain Mapp 1999b;8:272–284. [PubMed: 10619420]

Francis, WN.; Kucera, H. Frequency analysis of English usage: Lexicon and grammar. Houghton Mifflin; Boston: 1982.

Gold BT, Buckner RL. Common prefrontal regions coactivate with dissociable posterior regions during controlled semantic and phonological tasks. Neuron 2002;35:803–812. [PubMed: 12194878]

Hagler DJ Jr, Saygin AP, Sereno MI. Smoothing and cluster thresholding for cortical surface-based group analysis of fMRI data. Neuroimage 2006;33:1093–1103. [PubMed: 17011792]

Halgren E. How can intracranial recordings assist MEG source localization? Neurol Clin Neurophysiol 2004a;2004:86. [PubMed: 16012657]

Halgren E. How can intracranial recordings assist MEG source localization? Neurology and Clinical Neurophysiology 2004b;86:1–18.

Halgren E, Baudena P, Heit G, Clarke JM, Marinkovic K, Clarke M. Spatio-temporal stages in face and word processing. I. Depth-recorded potentials in the human occipital, temporal and parietal lobes [corrected]. J Physiol Paris 1994;88:1–50. [PubMed: 8019524]

Halgren E, Wang C, Schomer DL, Knake S, Marinkovic K, Wu J, Ulbert I. Processing stages underlying word recognition in the anteroventral temporal lobe. Neuroimage 2006;30:1401–1413. [PubMed: 16488158]

Hamalainen M, Hari R, Ilmoniemi RJ, Knuutila J, Lounasmaa OV. Magnetoencephalography--theory, instrumentation, and applications to noninvasive studies of the working human brain. Rev Mod Phys 1993;65:413–497.

Horner AJ, Henson RN. Priming, response learning and repetition suppression. Neuropsychologia 2008;46:1979–1991. [PubMed: 18328508]

Jenkinson M, Bannister P, Brady M, Smith S. Improved optimization for the robust and accurate linear registration and motion correction of brain images. Neuroimage 2002;17:825–841. [PubMed: 12377157]

Jenkinson M, Smith S. A global optimisation method for robust affine registration of brain images. Med Image Anal 2001;5:143–156. [PubMed: 11516708]

Jerbi K, Ossandon T, Hamame CM, Senova S, Dalal SS, Jung J, Minotti L, Bertrand O, Berthoz A, Kahane P, Lachaux JP. Task-related gamma-band dynamics from an intracerebral perspective: review and implications for surface EEG and MEG. Hum Brain Mapp 2009;30:1758–1771. [PubMed: 19343801]

Klaver P, Schnaidt M, Fell J, Ruhlmann J, Elger CE, Fernandez G. Functional dissociations in top-down control dependent neural repetition priming. Neuroimage 2007;34:1733–1743. [PubMed: 17178236]

Korsnes MS, Wright AA, Gabrieli JD. An fMRI analysis of object priming and workload in the precuneus complex. Neuropsychologia 2008;46:1454–1462. [PubMed: 18304592]

Lachaux JP, Fonlupt P, Kahane P, Minotti L, Hoffmann D, Bertrand O, Baciu M. Relationship between task-related gamma oscillations and BOLD signal: new insights from combined fMRI and intracranial EEG. Hum Brain Mapp 2007;28:1368–1375. [PubMed: 17274021]

Lachaux JP, Rodriguez E, Martinerie J, Varela FJ. Measuring phase synchrony in brain signals. Hum Brain Mapp 1999;8:194–208. [PubMed: 10619414]

Manning JR, Jacobs J, Fried I, Kahana MJ. Broadband shifts in local field potential power spectra are correlated with single-neuron spiking in humans. J Neurosci 2009;29:13613–13620. [PubMed: 19864573]

Marinkovic K, Dhond RP, Dale AM, Glessner M, Carr V, Halgren E. Spatiotemporal dynamics of modality-specific and supramodal word processing. Neuron 2003;38:487–497. [PubMed: 12741994]

Maris E, Oostenveld R. Nonparametric statistical testing of EEG- and MEG-data. J Neurosci Methods 2007;164:177–190. [PubMed: 17517438]

Matsumoto A, Iidaka T, Haneda K, Okada T, Sadato N. Linking semantic priming effect in functional MRI and event-related potentials. Neuroimage 2005;24:624–634. [PubMed: 15652298]

Oldfield RC. The assessment and analysis of handedness: the Edinburgh inventory. Neuropsychologia 1971;9:97–113. [PubMed: 5146491]

Oostendorp, TF.; Van Oosterom, A. Source parameter estimation using realistic geometry in bioelectricity and biomagnetism. In: Nenonen, J.; Rajala, HM.; Katila, T., editors. Biomagnetic Localization and 3D Modeling. Helsinki University of Technology; Helsinki: 1992. Report TKK-F-A689

Ostergaard AL. The effects on priming of word frequency, number of repetitions, and delay depend on the magnitude of priming. Mem Cognit 1998;26:40–60.

Pilgrim LK, Fadili J, Fletcher P, Tyler LK. Overcoming confounds of stimulus blocking: an event-related fMRI design of semantic processing. Neuroimage 2002;16:713–723. [PubMed: 12169255]

Schacter DL, Buckner RL. Priming and the brain. Neuron 1998;20:185–195. [PubMed: 9491981]

Scheibe C, Wartenburger I, Wustenberg T, Kathmann N, Villringer A, Heekeren HR. Neural correlates of the interaction between transient and sustained processes: a mixed blocked/event-related fMRI study. Hum Brain Mapp 2006;27:545–551. [PubMed: 16142781]

Sederberg PB, Schulze-Bonhage A, Madsen JR, Bromfield EB, McCarthy DC, Brandt A, Tully MS, Kahana MJ. Hippocampal and neocortical gamma oscillations predict memory formation in humans. Cereb Cortex 2007;17:1190–1196. [PubMed: 16831858]

Thompson-Schill SL, D'Esposito M, Aguirre GK, Farah MJ. Role of left inferior prefrontal cortex in retrieval of semantic knowledge: a reevaluation. Proc Natl Acad Sci U S A 1997;94:14792–14797. [PubMed: 9405692]

Wagner AD, Pare-Blagoev EJ, Clark J, Poldrack RA. Recovering meaning: left prefrontal cortex guides controlled semantic retrieval. Neuron 2001;31:329–338. [PubMed: 11502262]

Wagner AD, Shannon BJ, Kahn I, Buckner RL. Parietal lobe contributions to episodic memory retrieval. Trends Cogn Sci 2005;9:445–453. [PubMed: 16054861]

Weiss AP, Ellis CB, Roffman JL, Stufflebeam S, Hamalainen MS, Duff M, Goff DC, Schacter DL. Aberrant frontoparietal function during recognition memory in schizophrenia: a multimodal neuroimaging investigation. J Neurosci 2009;29:11347–11359. [PubMed: 19741141]

Whitham EM, Lewis T, Pope KJ, Fitzgibbon SP, Clark CR, Loveless S, DeLosAngeles D, Wallace AK, Broberg M, Willoughby JO. Thinking activates EMG in scalp electrical recordings. Clin Neurophysiol 2008;119:1166–1175. [PubMed: 18329954]

Woolrich MW, Ripley BD, Brady M, Smith SM. Temporal autocorrelation in univariate linear modeling of FMRI data. Neuroimage 2001;14:1370–1386. [PubMed: 11707093]

Worsley KJ, Marrett S, Neelin P, Vandal AC, Friston KJ, Evans AC. A unified statistical approach for determining significant signals in images of cerebral activation. Hum Brain Mapp 1996;4:58–73. [PubMed: 20408186]

Yuval-Greenberg S, Tomer O, Keren AS, Nelken I, Deouell LY. Transient induced gamma-band response in EEG as a manifestation of miniature saccades. Neuron 2008;58:429–441. [PubMed: 18466752]

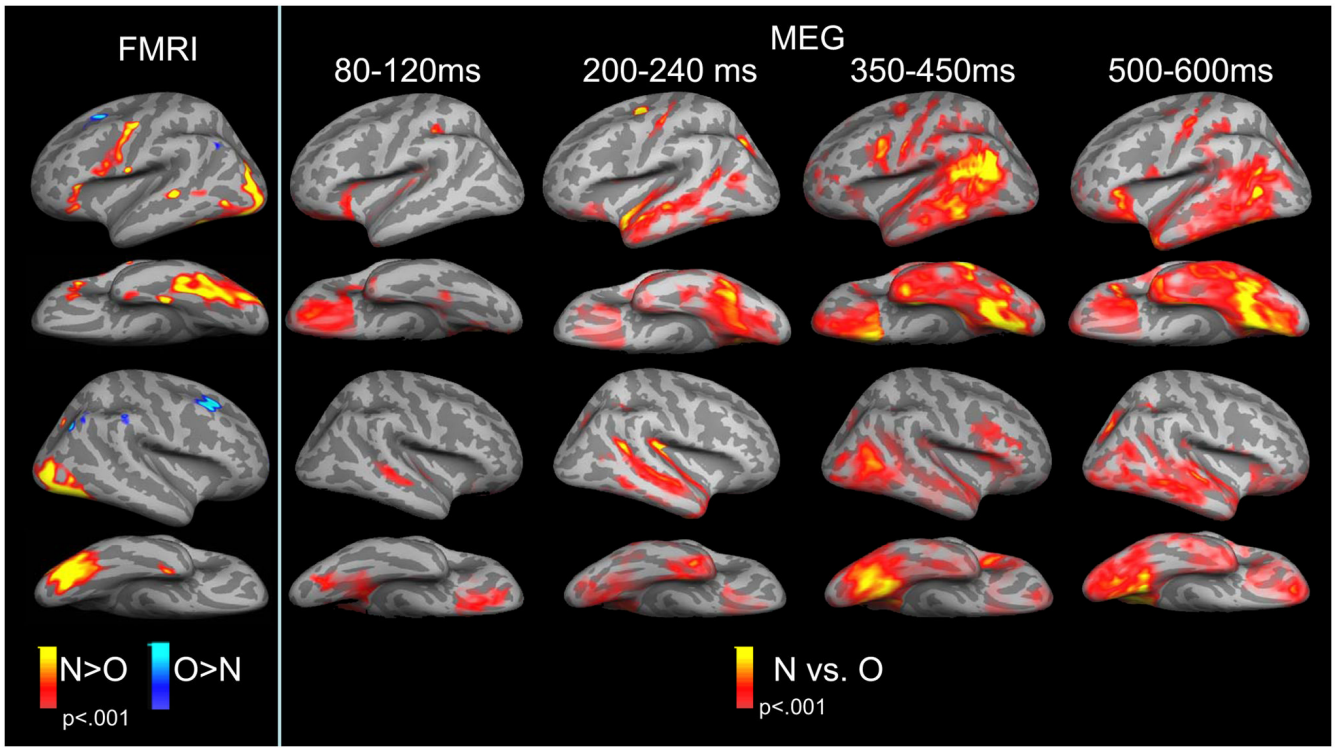

Figure 1.
Cluster-thresholded t-stat maps of the fMRI N > O (red/yellow) and O > N (cyan/blue) contrasts (left panel) and the MEG N vs O difference waveform for four time windows (right panel). Activity clusters are shown on the lateral and ventral inflated surfaces of both hemispheres (gyri = light gray; sulci = dark gray). Significance values range from a p<.001 to p <.00001 and represent significant clusters of activity exceeding a t-stat and size threshold.

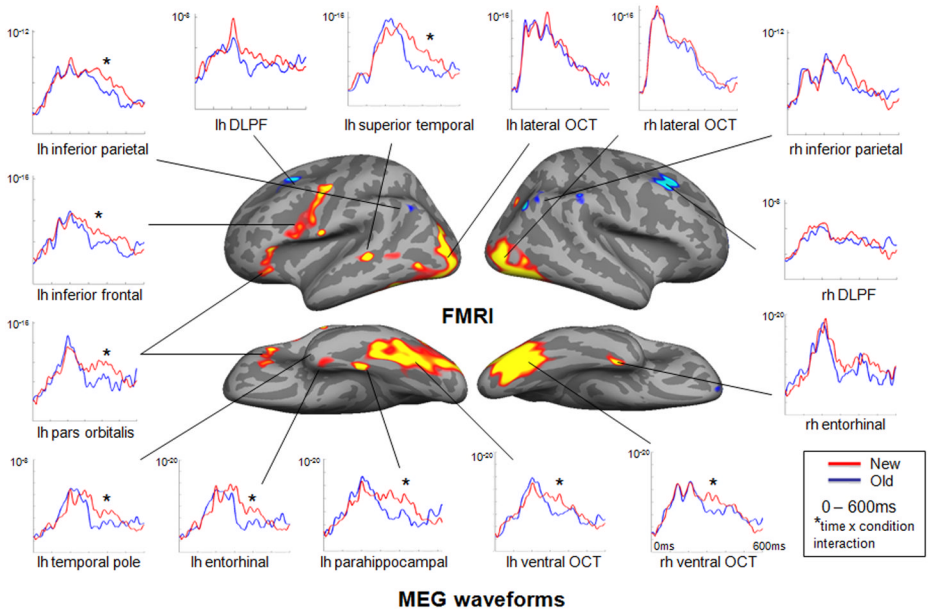

Figure 2.

fMRI cluster-thresholded t-stat maps of the N > O and O < N contrasts with MEG waveforms extracted from each significant fMRI cluster. MEG waveforms are shown from 0–600ms for new words (red) and old words (blue) within each ROI. Significance (*) denotes regions producing a condition x time interaction. Y-axis values reflect noise-normalized dipole strengths and can be conceptualized as estimates of the average signal-to-noise within an ROI.

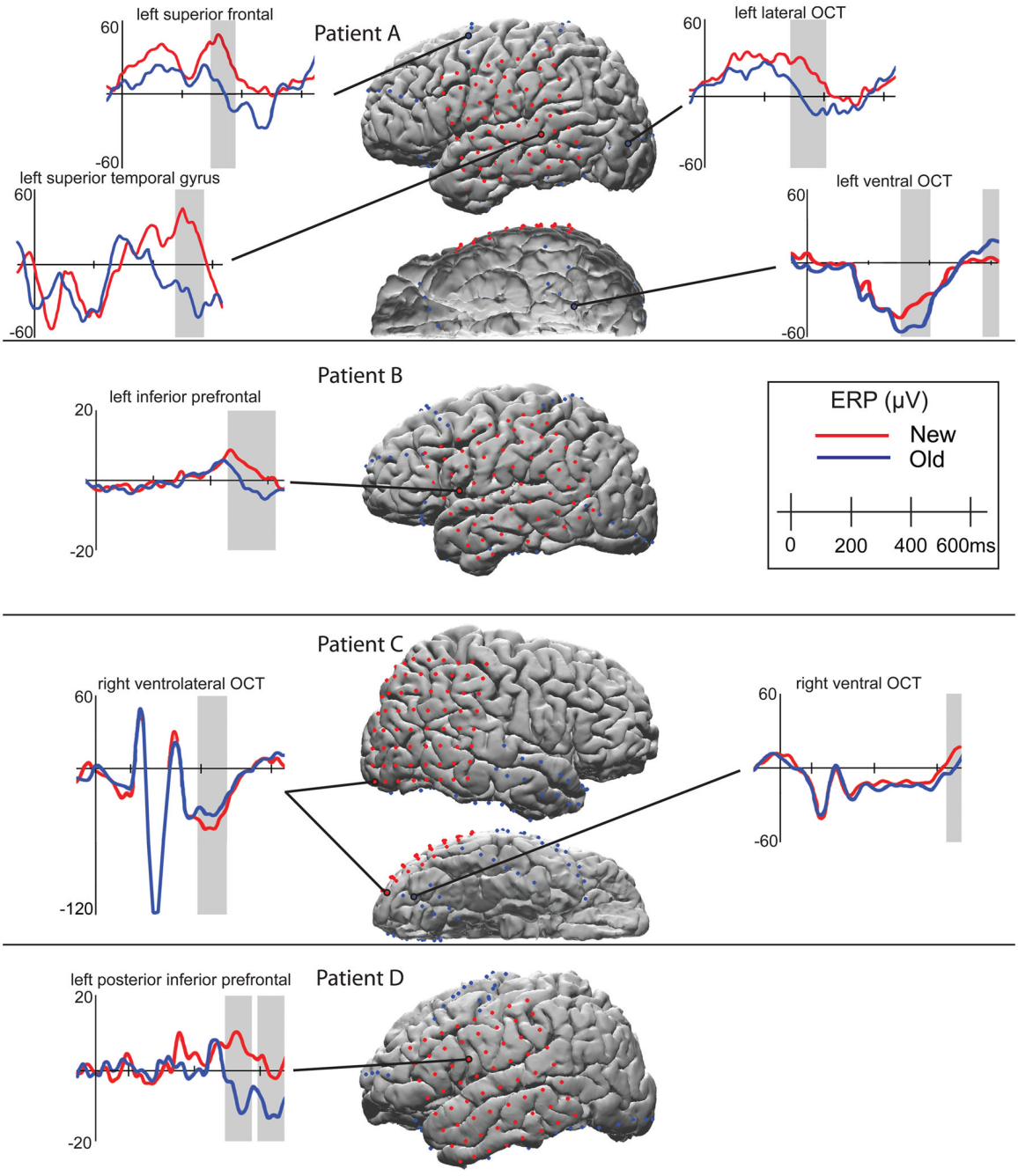

Figure 3.

Example ERPs from iEEG recordings in patients with intractable epilepsy. The y-axis represents the amplitudes (μV) of the N vs O words, scaled individually for each patient. Shaded areas reflect time windows during which N vs O words showed significantly different temporal clusters in the ERPs using randomization statistics. OCT = occipitotemporal.

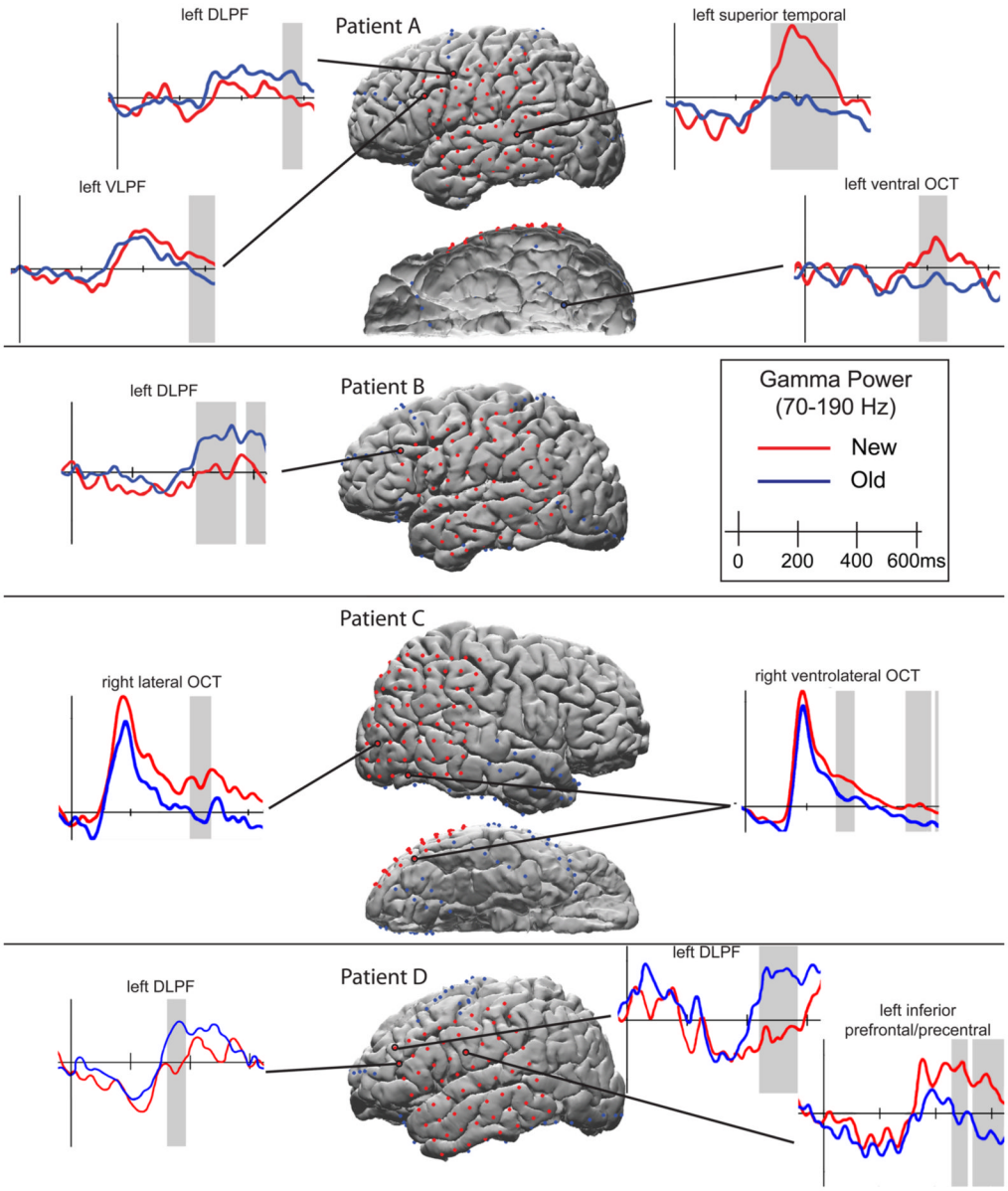

Figure 4.

Gamma power waves (integrated from 70–190 Hz) from iEEG recordings in patients with intractable epilepsy. The y-axis represents gamma power and is scaled for each plot to optimize visibility of the response. Shaded areas reflect time windows during which N vs O words showed significantly different temporal clusters in high gamma power using randomization statistics. OCT = occipitotemporal; DLPF = dorsolateral prefrontal; VLPF = ventrolateral prefrontal.

Table 1

Clinical Characteristics of the Patient Sample

Patient ID	Gender	Age	Age of seizure onset	Handedness	Seizure Localization	MRI	Surgery
Patient A	Male	26	15	Right	Left MTL	Left MTS	Left ATL
Patient B	Female	53	32	Right	Left MTL	Left MTS	Left ATL
Patient C	Male	42	13	Right	Right MTL	Normal	Right ATL
Patient D	Female	44	4	Right	Left MTL	Left MTS	Left ATL
Patient E	Male	53	12	Right	Left OTL	Normal	Left occipital resection
Patient F	Male	18	7	Right	Right MTL	Left HC atrophy	Right ATL

MTL = mesial temporal lobe; OTL = occipitotemporal lobe; HC = hippocampal

Table 2

Average Percent Signal Change for Each Region of Interest

Region of interest	Mean % signal change (standard deviation)	Range of % signal change
N > O		
Left entorhinal	.16 (.05)	.10 – .23
Left ventral occipitotemporal	.14 (.04)	.08 – .21
Left posterior inferior frontal	.16 (.04)	.10 – .23
Left superior temporal	.15 (.03)	.11 – .20
Left middle temporal	.15 (.04)	.11 – .24
Left pars orbitalis	.14 (.04)	.09 – .21
Left parahippocampal	.16 (.03)	.11 – .21
Left lateral occipital	.16 (.04)	.11 – .22
Left superior medial frontal	.19 (.02)	.09 – .24
Right entorhinal	.13 (.03)	.08 – .21
Right ventral occipitotemporal	.14 (.03)	.10 – .20
Right lateral occipitotemporal	.14 (.03)	.10 – .19
O > N		
Left dorsolateral prefrontal	.15 (.03)	.10 – .20
Left inferior parietal	.15 (.04)	.10 – .23
Left precuneus	.14 (.04)	.10 – .22
Right dorsolateral prefrontal	.14 (.04)	.10 – .20
Right inferior parietal	.14 (.03)	.09 – .20
Right precuneus	.13 (.03)	.10 – .18

Table 3

Neocortical regions showing repetition effects in MEG and iEEG ERP and high gamma responses

Region of interest	350–450			500–600		
	MEG	ERP	70+ Hz	MEG	ERP	70+ Hz
Left						
Dorsolateral Prefrontal		1/4	2/4		1/4	3/4*
Inferior Frontal	X	2/3	0/3		2/3	1/3
Lateral Occipitotemporal		2/4	2/4		1/4	1/4*
Ventral Occipitotemporal	X	2/4	2/4		0/4	0/4
Superior Medial Frontal		1/2	0/2		0/2	1/2*
Superior Temporal	X	2/4	1/4		1/4	1/4*
Right						
Dorsolateral Prefrontal		0/1	0/1		1/1	0/1
Lateral Occipitotemporal	X	1/1	1/1		0/4	1/4*
Ventral Occipitotemporal	X	2/2	2/2		2/2	0/2

*reflects increases in gamma power to O vs N words. All other responses in the 70+ Hz analysis reflect increases to N vs O gamma power.

Table 4

Neocortical regions showing significant repetition effects in each modality

Region of interest	fMRI	MEG 350–450ms	iEEG[+] 350–450ms
Left			
Temporal Pole		X	
Dorsolateral prefrontal	X[*]		X
Entorhinal	X	X	
Inferior Frontal[**]	**X**	**X**	**X**
Lateral Occipitotemporal	X		X
Ventral Occipitotemporal	**X**	**X**	**X**
Middle Temporal	X	X	
Parahippocampal	X	X	
Pars Orbitalis	X	X	
Supramarginal	X[*]	X	
Superior Medial Frontal	X		X
Superior Temporal	**X**	**X**	**X**
Temporoparietal		X	
Right			
Dorsolateral prefrontal	X[*]		
Entorhinal	X		
Lateral Occipitotemporal	**X**	**X**	**X**
Ventral Occipitotemporal	**X**	**X**	**X**
Supramarginal	X[*]		

[*] Regions showing O > N effects. All other regions represent those showing N > O effects.

[+] Regions in which one or more patients showed a significant iEEG repetition effect. The absence of an effect in the iEEG column does not necessary represent discordance, but may reflect inadequate grid coverage or the elimination of electrodes in which interictal activity was detected.

[**] Bolded regions are those demonstrating concordance across all three modalities.